Thermo Elastic Analysis of Carbon Nanotube-Reinforced Composite Cylinder Utilizing Finite Element Method with the Theory of Elasticity

Hamad Mohammed Hasan
Lecturer
Engineering College -Al-Anbar University
hamad1971h@yahoo.com

ABSTRACT

In this paper, the axisymmetric bending behavior of FG_CNTRC moderately thick cylinder under the effect of internal pressure and thermal load is investigated. Three kinds of distributions of a single-walled carbon nanotube (SWCNT) are utilized, that is uniform and two types of functionally graded distributions of CNTs through the radial direction of cylinder. The governing equations are derived based on the elasticity theory. The steady state heat conduction with convection heat transfer on the inner surface of cylinder and the thermo elastic equations are solved numerically by the finite element method. A computer program by Fortran95 (FTN95) has been built to obtain the temperature distribution and displacement field through the radial and longitudinal direction of the cylinder. In detail, parametric studies have been achieved to show the effect of convection heat transfer coefficient and the kind of CNTs distributions on the bending response of the cylinder. It's found that the percentage increasing in the radial displacement (Ur) about (34%), when the value of conduction heat transfer coefficient increase from (hc=5 W/m^2 K) to (hc=5 W/m^2 K). Also, it's found that, the value of (Ur = 0.15) for FG_V as compared with the value (Ur = 0.1) for the FG_X distribution. Moreover, the influence of various boundary conditions is also investigated. The accuracy of the current study is validated by comparative study with that available in the literature and found that the percentage error between two studies in the range of (0.022%, 0.042%, and 0.047%) for UD, FG_V and FG_X distribution respectively. So, there is a good agreement for the results.

Keywords: carbon nanotube, convection, finite element, theory of elasticity, fortran95.

التحليل الحراري والمرن للانابيب المركبة والمقواة بالياف الكاربون المتناهية بالصغر باستخدام طريقة العناصر المحددة ونظرية المرونة

حمد محمد حسن
مدرس
كلية الهندسة – جامعة الانبار

الخلاصة

في هذا البحث تمت دراسة الانحناء المتناضر للانابيب المعززة بألياف الكاربون ذات الخواص المتغيرة تدريجيا تحت تاثير الضغط الداخلي للانبوب والحمل الحراري . ثلاث انواع من التوزيع لالياف الكاربون تمت دراستها هما التوزيع المنتظم واثنان من التوزيع المتدرج خلال الاتجاه القطري للانبوب .تم اشتقاق المعادلات الحاكمة للحركة بالاستناد الى نظرية المرونة .تم استخدام طريقة العناصر المحددة لحل معادلات انتقال الحرارة عدديا. تم بناء برنامج بواسطة لغة الفورتون لبيان توزيع درجات الحرارة والتشوهات خلال الاتجاه القطري والطولي للانبوب . تم انجاز دراسة تفصيلية لبيان تاثير معامل الحمل الحراري وكذلك تاثير انواع توزيع الياف الكاربون على استجابة الانحناء للانبوب وكذلك تمت دراسة تاثير انواع الاسناد للانبوب (boundary conditions) . تم اجراء دراسة مقارنة مع الدراسات السابقة لبيان دقة صحة الدراسة ووجد هناك تقارب كبير بين النتائج لكلا الدراستين .

الكلمات الرئيسية : كاربون نانوتيوب ، الحمل الحراري ، العناصر المحددة ، نظرية المرونة ، فورتران 95 .

1. INTRODUCTION

Since the beginning of the last decade, carbon nanotubes have become the focus of significant research, **Lau,and Hui, 2002, Thostenson,et al.,2001** The excellent physical and mechanical properties encourage the researchers to concentrate on this kind of materials. From the unparalleled electrical properties, thermal conductivity higher than diamond to mechanical characteristics, where the stiffness and strength override any present material, **Liu ,andChen,2003**. **Qian, et al.,2000** Many studies of carbon nanotubes-reinforced composites (CNTRCs) have been concentrated on the composite properties. **Seidel, et al.,2006** evaluated the effective mechanical properties of CNTs in two step process by using composite cylinders micromechanics method as initial step and then the elastic properties of composites calculated by utilizing Mori-Tanaka technique. **Hu, et al. 2005** presented the macroscopic elastic properties of carbon nanotubes reinforced composites by analyzing the elastic distortion of a representative volume element. Many of researches have displayed that the addendum of little quantities of carbon nanotubes can significantly get better the mechanical and thermal properties of the composites which reinforced by carbon nanotubes , **Yang, et al., 2011, Manchado, et al., 2005** . Although these researches are perfectly helpful in foundress the performance behavior of the Nano composites, their utilization in veritable structural applications is the main target for the improvement for this kind of advanced materials. So, the first study on the actual nanocomposites reinforced by CNTs was achieved by ,**Vodenitcharova, and Zhang,2006**. They investigated the pure bending and local buckling of the nanocomposite beam reinforced by single-walled carbon nanotube. With the multiscale analysis, the stress and deflection behavior for the carbon nanotubes reinforced composite beam is investigated by ,**Wuite ,and Adali, 2005**. Their outcome proved that, the enforcement by adding a little portion of CNTs produce a considerable improvement in beam toughness.

Shen,2009 used the perturbation method to investigate the nonlinear bending behavior of functionally graded carbon nanotubes reinforced composite plate under the effect of mechanical and thermal loads. His results revealed that, the temperature rise has a great influence on the bending behavior of the composite plates. Also, the same author investigated the postbuckling of the composite cylindrical shell reinforced by carbon nanotubes under the influence of torsion with thermal conditions **Shen,2014**. His results showed that the buckling torque can be increased with the linear functionally graded reinforcements.

Based on the element-free Ritz technique, **Lei et al. 2013**, presented the buckling behavior of functionally graded carbon nanotubes reinforced composite plates under the effect of different in plane mechanical loads. Their results proved that, the distribution kind of carbon nanotubes, geometric parameters and loading conditions have considerable effects on the buckling loads. Furthermore, **Lei et al.,2013,** performed the nonlinear deflection behavior of composite plates strengthened by single-walled carbon nanotubes. Their outcome revealed that, the nonlinear performance of the nanocomposite plates affected by the distribution types and volume fractions of the carbon nanotubes.

By depending on the finite element method, **Ping et al.,2012**, carried out the bending and free vibration behavior of composite plates strengthened by carbon nanotubes. Their steady revealed that, the volume fraction of the carbon nanotube has a great influence on the bending behavior, but it's not effect on the central axial stress and free vibration. The behavior of nonlinear vibration for the cylindrical shells reinforced by carbon nanotubes under the effect of thermal environment was studied by ,**Shen, and Xiang, 2011**. Their study depends on the perturbation method in order to obtain the nonlinear frequencies and it concluded that the

temperature rise has a great effect on the natural frequencies of the composite plates. Based on the mesh-free technique, the transient and free vibration behavior of nanocomposite cylinders reinforced by carbon nanotubes was investigated by **Rasool et al. 2013**.Their investigations revealed that the volume fraction of carbon nanotubes and geometric parameter have a great influence on the dynamic response of the nanocomposite cylinder. Under the effect of mechanical loads, the large deflection of functionally graded carbon nanotubes reinforced cylindrical panels was analyzed by **Zhang et al. 2014**. Their study used mesh-free kp-Ritz technique with the modified Newton-Raphson method to resolve the system of nonlinear equations. Furthermore, **Malekzadeh et al., 2012**, investigated the effect of convection heat transfer on the transient behavior of rotating laminated functionally graded cylindrical shells. Their study utilized differential quadrature method and found that the convection heat transfer coefficient has a great influence on the behavior of the functionally graded cylindrical shell.

Finally, the three-dimensional elasticity theory used by **Alibeigloo, and Liew,2013** to investigate the bending behavior of the FG-CNT reinforced composite plate under the action of thermal and mechanical loads. Their study utilized Fourier series expansion and state space method to evaluate the exact solution for plate bending. They found that, the temperature difference near the bottom surface has a significant influence on the bending behavior.

It is clear that, the thermo-elastic behavior of functionally graded carbon nanotubes reinforced cylinders under the effect of convection heat transfer has not been yet studied and the present work endeavors to consider this analysis.

2. CARBON NANOTUBES REINFORCED COMPOSITE CYLINDERS

Consider a composite cylinder of length l , inner and outer radius of r_{in} and r_{ou} respectively. It is assumed that, the cylinder fabricated from a mishmash of single-walled carbon nanotubes along the longitudinal direction and an isotropic polymer.

The effective material properties for the constituent's mixture of the carbon nanotubes and the polymer can be evaluated by using either the rule of mixture or the Mori-Tanaka method. Because of suitability and straightforward, the present study utilized the rule of mixture. The effective mechanical and thermal properties of CNTs reinforced cylinders can be written as **Alibeigloo, and Liew,2013:**

$$E_{11} = \eta_1 V_{cn} E_{11}^{cn} + V_m E^m \tag{1a}$$

$$\frac{\eta_2}{E_{22}} = \frac{V_{cn}}{E_{22}^{cn}} + \frac{V_m}{E^m} \tag{1b}$$

$$\frac{\eta_3}{G_{12}} = \frac{V_{cn}}{G_{12}^{cn}} + \frac{V_m}{G^m} \tag{1c}$$

$$\nu_{ij} = V_{cn}\nu_{ij}^{cn} + V_m\nu^m \qquad i,j=1,2,3 \;\&\; i \neq j \tag{1d}$$

$$\alpha_{11} = V_{cn}\alpha_{11}^{cn} + V_m\alpha^m \tag{1e}$$

$$\alpha_{22} = (1+\nu_{12}^{cn})V_{cn}\alpha_{22}^{cn} + (1+\nu_m)V_m\alpha^m - \nu_{12}\alpha_{11} \tag{1f}$$

in order to calculate for the scale dependent material properties, $\eta_j\,(j=1,2,3)$, the carbon nanotube efficiency parameters were inserted and can be evaluated by matching the effective properties of carbon nanotube from the molecular dynamic simulation together with the numerical results evaluated from the rule of mixture.

The distribution form of the carbon nanotube volume fraction has significant influence on the composite cylinder behavior. So, in the present study three kinds of CNT volume fraction distributions are considered in the radial direction of the cylinder as shown in **Fig.1**. The first type UD clarifies the uniform distribution and the other two (FG_V, FG_X) the functionally graded distribution in the radial direction of the cylinder. The mathematical models for the above distribution are as follow, **Alibeigloo, and Liew,2013**:

$$Model\ FG\_V: V_{cn} = 2\left(\frac{r_{ou} - r}{r_{ou} - r_{in}}\right)V_{cn}^{*} \tag{2a}$$

$$Model\ FG\_X: V_{cn} = 4\left|\frac{r - r_m}{r_{ou} - r_{in}}\right|V_{cn}^{*} \tag{2b}$$

$$Model\ \ UD\ \ \ : V_{cn} = V_{cn}^{*} \tag{2c}$$

where

$$V_{cn}^{*} = \frac{W_{cn}}{W_{cn} + \left(\frac{\rho_{cn}}{\rho_m}\right) - \left(\frac{\rho_{cn}}{\rho_m}\right)W_{cn}} \tag{2d}$$

3. MATHEMATICAL MODELING

The inner surface of CNTRC cylinder is assumed to be subjected to a convection heat transfer and internal pressure but the outer surface is free from mechanical loading and has a constant temperature. Because of the axisymmetric geometry and loading conditions of CNTRC cylinder, the thermoelastic equations decrease to the two-dimensional ones. According to that, a cylindrical coordinate system (r, z) is suitable to represent the un deformed points of the CNTRC cylinder.

The steady state in (r, z) coordinates, heat conduction equation for each of the three models of CNTRC distribution along radial and longitudinal directions is considered as **Shen, and Xiang, 2011**:

$$-\left[\frac{1}{r}k_r\frac{\partial}{\partial r}\left(r\frac{\partial T}{\partial r}\right) + k_z\frac{\partial}{\partial z}\left(\frac{\partial T}{\partial z}\right)\right] = 0 \qquad For\ UD \tag{3a}$$

$$-\left[\frac{1}{r}k_r(r)\frac{\partial}{\partial r}\left(r\frac{\partial T}{\partial r}\right) + k_z(r)\frac{\partial}{\partial z}\left(\frac{\partial T}{\partial z}\right)\right] = 0 \qquad For\ FG \tag{3b}$$

Also, the thermal conductivity for each case of CNTRC cylinder distribution is

$$k_i = 1 + 2D_i\left(\frac{r - r_{in}}{r_{ou} - r_{in}}\right) \qquad for\ \ FG \qquad (4a)$$

$$k_i = 1 + D_i \qquad for\ \ UD \qquad (4b)$$

$$Where \qquad D_i = \frac{PV_{cn}^*}{3} * \frac{\frac{k_i^{cn}}{k_m}}{P + \frac{2a_k k_i^{cn}}{dk_m}} \quad , \ (i = r, z) \qquad (4c)$$

The thermal and displacement boundary conditions are, **Malekzadeh et al., 2012**:

$$k_r \frac{\partial T}{\partial r} + h_c\left(T - T_\infty\right) = 0 \qquad at\ r = r_{in} \qquad (5a)$$

$$T = T_0 \qquad at\ r = r_{ou} \qquad (5b)$$

$$u_r(r,0) = u_r(r,l) = u_z(r,0) = u_z(r,l) = 0 \qquad for\ clamped - clamped \qquad (5c)$$

$$u_r(r,0) = u_z(r,0) = 0 \qquad for\ clamped - free \qquad (5d)$$

3.1 Finite element solution for temperature field

The weak form for Eq. (3), **Reddy JN. 2006**.

$$2\pi \int_\Omega \lambda \left[-\left(\frac{1}{r} k_r(r) \frac{\partial}{\partial r}\left(r \frac{\partial T}{\partial r} \right) + k_z(r) \frac{\partial}{\partial z}\left(\frac{\partial T}{\partial z} \right) \right) \right] r dr dz = 0 \qquad (6a)$$

$$2\pi \int_\Omega \left(k_r \frac{\partial \lambda}{\partial r}\frac{\partial T}{\partial r} + k_z \frac{\partial \lambda}{\partial z}\frac{\partial T}{\partial z} \right) r dr dz - 2\pi \int_\Gamma \lambda k_r \frac{\partial T}{\partial r} ds = 0 \qquad (6b)$$

From Eq. (5a)

$$k_r \frac{\partial T}{\partial r} = -h_c\left(T - T_\infty\right) \qquad (7a)$$

$$2\pi \int_\Omega \left(k_r \frac{\partial \lambda}{\partial r}\frac{\partial T}{\partial r} + k_z \frac{\partial \lambda}{\partial z}\frac{\partial T}{\partial z} \right) r dr dz - 2\pi \int_\Gamma \left(\lambda\left(-h_c\left(T - T_\infty\right) \right) \right) ds = 0 \qquad (7b)$$

$$2\pi \int_\Omega \left(k_r \frac{\partial \lambda}{\partial r}\frac{\partial T}{\partial r} + k_z \frac{\partial \lambda}{\partial z}\frac{\partial T}{\partial z} \right) r dr dz + 2\pi \int_\Gamma \lambda h_c T ds = 2\pi \int_\Gamma \lambda h_c T_\infty ds \qquad (7c)$$

The finite element model of Eq. (6c) is obtained by substituting the finite element approximation of the form

$$T(r,z)=\sum_{j=1}^{n}T_j^e\varphi_j^e(r,z) \tag{8}$$

And φ_i for λ into Eq. (6c)

$$\sum\left(K_{ij}^e+H_{ij}^e\right)T_j^e=P_i^e \tag{9}$$

where

$$K_{ij}^e=2\pi\int_{\Omega}\left(k_r(r)\frac{\partial\varphi_i^e}{\partial r}\frac{\partial\varphi_j^e}{\partial r}+k_z(r)\frac{\partial\varphi_i^e}{\partial z}\frac{\partial\varphi_j^e}{\partial z}\right)rdrdz \tag{10a}$$

$$H_{ij}^e=2\pi\int_{\Gamma}h_c^e\varphi_i^e\varphi_j^e ds \tag{10b}$$

$$P_i^e=2\pi\int_{\Gamma}h_c^e\varphi_i^eT_\infty^e ds \tag{10c}$$

3.2 Finite element solution for displacement field

The equilibrium equations of motion in the cylindrical coordinate system for CNTRC cylinder are given as:

$$\frac{\partial\sigma_z}{\partial z}+\frac{\partial\tau_{rz}}{\partial r}+\frac{1}{r}\tau_{rz}=0 \tag{11a}$$

$$\frac{\partial\tau_{rz}}{\partial z}+\frac{\partial\sigma_r}{\partial r}+\frac{1}{r}(\sigma_r-\sigma_\theta)=0 \tag{11b}$$

The linear stress-strain relations with heat conduction equations for CNTRC cylinder are given by:

$$\begin{pmatrix}\sigma_z\\ \sigma_r\\ \sigma_\theta\\ \tau_{rz}\end{pmatrix}=\begin{pmatrix}c_{11} & c_{12} & c_{13} & 0\\ c_{12} & c_{22} & c_{23} & 0\\ c_{13} & c_{23} & c_{33} & 0\\ 0 & 0 & 0 & c_{55}\end{pmatrix}\begin{pmatrix}\varepsilon_z-\alpha_zT\\ \varepsilon_r-\alpha_rT\\ \varepsilon_\theta\\ \gamma_{rz}\end{pmatrix} \tag{12}$$

The linear strain-displacement relations are

$$\varepsilon_z=\frac{\partial u_z}{\partial z},\varepsilon_r=\frac{\partial u_r}{\partial r},\varepsilon_\theta=\frac{1}{r}u_r \tag{13a}$$

$$\gamma_{rz}=\frac{\partial u_z}{\partial r}+\frac{\partial u_r}{\partial z} \tag{13b}$$

The weak form for the equilibrium equations (11)

$$\int_{\Omega}\left(\lambda\frac{\partial\sigma_z}{\partial z}+\lambda\frac{\partial\tau_{rz}}{\partial r}+\lambda\frac{1}{r}\tau_{rz}\right)rdrd\theta dz=0 \tag{14a}$$

$$\int_{\Omega}\left(\lambda\frac{\partial\tau_{rz}}{\partial z}+\lambda\frac{\partial\sigma_r}{\partial r}+\lambda\frac{1}{r}(\sigma_r-\sigma_\theta)\right)rdrd\theta dz=0 \tag{14b}$$

By integrating by parts and utilizing Gauss's divergence theorem

$$2\pi\int_{\Omega}-\left(\frac{\partial\lambda}{\partial z}\sigma_z+\frac{\partial\lambda}{\partial r}\tau_{rz}\right)rdrdz+2\pi\int_{\Gamma}\lambda\sigma_z\hat{n}_z rdr+2\pi\int_{\Gamma}\lambda\tau_{rz}\hat{n}_r rdz=0 \qquad (15a)$$

$$2\pi\int_{\Omega}-\left(\frac{\partial\lambda}{\partial z}\tau_{rz}+\frac{\partial\lambda}{\partial r}\sigma_r+\lambda\frac{1}{r}\sigma_\theta\right)rdrdz+2\pi\int_{\Gamma}\lambda\tau_{rz}\hat{n}_z rdr+2\pi\int_{\Gamma}\lambda\sigma_r\hat{n}_r rdz=0 \qquad (15b)$$

The boundary integrals denote the forces acting on the element face.

By substituting Eq. (12) and Eq.(13) into Eq. (14)

$$2\pi\int_{\Omega}\left(c_{11}r\frac{\partial\lambda}{\partial z}\frac{\partial u_z}{\partial z}+c_{55}r\frac{\partial\lambda}{\partial r}\frac{\partial u_z}{\partial r}+c_{12}r\frac{\partial\lambda}{\partial z}\frac{\partial u_r}{\partial r}+c_{13}\frac{\partial\lambda}{\partial z}u_r+c_{55}r\frac{\partial\lambda}{\partial r}\frac{\partial u_r}{\partial z}\right)drdz-$$
$$2\pi\int_{\Omega}Tr\left(c_{11}\frac{\partial\lambda}{\partial z}\alpha_z+c_{12}\frac{\partial\lambda}{\partial z}\alpha_r\right)drdz=0 \qquad (16a)$$

$$2\pi\int_{\Omega}\left(c_{55}r\frac{\partial\lambda}{\partial z}\frac{\partial u_z}{\partial r}+c_{12}r\frac{\partial\lambda}{\partial r}\frac{\partial u_z}{\partial z}+c_{13}r\lambda\frac{\partial u_z}{\partial z}+c_{55}r\frac{\partial\lambda}{\partial z}\frac{\partial u_r}{\partial z}+c_{22}r\frac{\partial\lambda}{\partial r}\frac{\partial u_r}{\partial r}+c_{23}\frac{\partial\lambda}{\partial r}u_r+c_{23}\lambda\frac{\partial u_r}{\partial r}+c_{33}\frac{1}{r}\lambda u_r\right)drdz-$$
$$2\pi\int T\left(r\frac{\partial\lambda}{\partial r}\left(c_{12}\alpha_z+c_{22}\alpha_r\right)+\lambda\left(c_{13}\alpha_z+c_{23}\alpha_r\right)\right)drdz=0 \qquad (16b)$$

So, the finite element model of Eq. (16) is obtained by substituting the finite element approximation of the form

$$u_z=\sum_{j=1}^{n}\varphi_j u_z^j \quad , \; u_r=\sum_{j=1}^{n}\varphi_j u_r^j \quad , \quad \lambda=\sum_{j=1}^{n}\varphi_i \qquad (17)$$

So, equations (16) becomes

$$2\pi\int_{\Omega}\left(\left(c_{11}r\frac{\partial\varphi_i}{\partial z}\frac{\partial\varphi_j}{\partial z}+c_{55}r\frac{\partial\varphi_i}{\partial r}\frac{\partial\varphi_j}{\partial r}\right)u_z^j+\left(c_{12}r\frac{\partial\varphi_i}{\partial z}\frac{\partial\varphi_j}{\partial r}+c_{13}\frac{\partial\varphi_i}{\partial z}\varphi_j+c_{55}r\frac{\partial\varphi_i}{\partial r}\frac{\partial\varphi_j}{\partial z}\right)u_r^j-\right.$$
$$\left.Tr\left(c_{11}\frac{\partial\varphi_i}{\partial z}\alpha_z+c_{12}\frac{\partial\varphi_i}{\partial z}\alpha_r\right)\right)drdz \qquad (18a)$$

$$2\pi\int_{\Omega}\left(\left(c_{55}r\frac{\partial\varphi_i}{\partial z}\frac{\partial\varphi_j}{\partial r}+c_{12}r\frac{\partial\varphi_i}{\partial r}\frac{\partial\varphi_j}{\partial z}+c_{13}\varphi_i\frac{\partial\varphi_j}{\partial z}\right)u_z^j+\left(c_{55}r\frac{\partial\varphi_i}{\partial z}\frac{\partial\varphi_j}{\partial z}+c_{22}r\frac{\partial\varphi_i}{\partial r}\frac{\partial\varphi_j}{\partial r}+c_{23}\frac{\partial\varphi_i}{\partial r}\varphi_j+\right.\right.$$
$$\left.\left.c_{23}\varphi_i\frac{\partial\varphi_j}{\partial r}+c_{33}\frac{1}{r}\varphi_i\varphi_j\right)-T\left(r\frac{\partial\varphi_i}{\partial r}\left(c_{12}\alpha_z+c_{22}\alpha_r\right)+\varphi_i\left(c_{13}\alpha_z+c_{23}\alpha_r\right)\right)\right)drdz=0 \qquad (18b)$$

The integrals can be represented in matrix form

$$[K]\{d\}=\{R\} \tag{19a}$$

$$\begin{bmatrix} K_{ij}^{11} & K_{ij}^{12} \\ K_{ij}^{21} & K_{ij}^{22} \end{bmatrix} \begin{Bmatrix} u_z^i \\ u_r^i \end{Bmatrix} = \begin{Bmatrix} R_z^i \\ R_r^i \end{Bmatrix} \tag{19b}$$

4. NUMERICAL RESULTS AND DISCUSSION

In the following, numerical results are utilized to display the veracity and the influence of convection heat transfer on the thermo-elastic response of nanocomposite cylinder. The mechanical, thermal properties of CNT and matrix polymer are written in table1. With a view to validate the current work, a comparative study for the dimensionless transverse displacement of CNTRC plate under the effect of pressure load, in three cases of CNT distributions with those available in the open literature are written in Table 2. Since the bending behavior in Ref. **Ping et al.,2012**, is solved numerically by finite element method as in the present study, the results are very close to each other.

Through the present study, CNTRC cylinder considered with inner radius, r_{in}=0.4m, and outer radius r_{ou}=0.5m. In addition, the values of internal pressure $\left(P_{in}=-1MPa\right)$ applied on the inner surface of cylinder, $T_0=300(K), T_\infty=1100(K), V_{cn}^*=0.17, l=1\,m$ are used in the case study. The dimensionless quantities included $U_r=-\frac{u_r}{r_{ou}-r_{in}}, U_z=\frac{u_z}{l}, R=\frac{r-r_{in}}{r_{ou}-r_{in}}$ are used to represent the results. **Fig.2** shows the temperature distribution through the radial direction of the CNTRC cylinder. According to this figure, the temperature distribution through the radial direction increases as the convection heat transfer coefficient increase. Also, it is clear that, the temperature distribution is linearly, because the formula for the thermal conductivity varying linearly through the radial and longitudinal direction of cylinder. For more debate, numerical investigations have been executed for clamped-clamped and clamped-free boundary conditions illustrated in **Figs.3-8** describe the influence of convection heat transfer coefficient and the type of carbon nanotube distribution on the cylinder behavior.

Fig3a-c shows the effect of the convection heat transfer coefficient on transverse displacement for three types of CNT distribution. From this figure, it is obviously that the value of transverse displacement has maximum value on the inner surface of the cylinder. This is due to the inner surface has maximum value of thermal and mechanical loads. Also, it is clear that the increasing in the convection heat transfer coefficient lead to increase the transverse displacement. **Fig.4** describes the effect of type of carbon nanotube distribution on transverse displacement through radial direction. It is clear that, the transverse displacement in the case of FG_X has minimum value, while as it is maximum in the case of FG_V CNT distribution. Furthermore, **Fig.5** depicts the behavior of the transverse displacement through the longitudinal direction of the cylinder under the effect of type of carbon nanotube distribution and convection heat transfer coefficient.

For clamped-free condition, the behavior of CNTRC cylinder is different from clamped-clamped condition. As shown in **Fig.6** which shows the behavior of transverse displacement through radial direction for three types of CNT distribution. It is seen that, the uniform distribution (UD) has the maximum value as it is minimum in the condition of functionally graded and according to that the numerical results are for the condition of FG_X distribution. Furthermore, **Fig.7a-C** illustrates the effect of convection heat transfer coefficient on transverse displacement in radial direction for three kinds of CNT distribution. Also as in

clamped-clamped condition, it is seen that the increasing in convection heat transfer coefficient lead to increase in transverse displacement for all three types of CNT distribution, but the response of transverse displacement in case of clamped-free is higher than that for the first condition.

Finally, **Fig.8a-c** presents the behavior of longitudinal displacement through the radial direction for different types of CNT distribution and convection heat transfer coefficient. From this fig. it is clear that the CNT distribution plays an important role in the behavior of longitudinal displacement and also the convection heat transfer coefficient has the same effect.

5. CONCLUSION

The axisymmetric bending behavior of functionally graded CNTRC cylinder under the effect of thermal and internal pressure has been analyzed. Also in this study it has been programming the finite element method by FTN95 to solve the temperature field and displacement. The effect of convection heat transfer coefficient as well as the type of CNT distribution on thermoelastic behavior of functionally graded CNTRC cylinder was investigated. It is concluded that, the convection heat transfer coefficient and the type of CNT distribution has a great effect on the behavior of cylinder. From the study, some remarkable conclusions can be written.

- The influence of FG_V distribution on the displacement field is more significant than that for the other kinds of distribution.
- Effect of increasing convection heat transfer coefficient (hc) on the radial displacement in the case of FG_V distribution is more significant than that for the other kinds of distribution.
- The effect of clamped-free condition on the response of the CNTRC cylinder is greater than the influence of clamped-free condition.
- The deformation on the inner surface of the cylinder (Uz) is higher than that on the outer surface in case of FG_V distribution, while it remains constant in the case of FG_X and UD distributions.
- The influence of increasing the convection heat transfer coefficient is significant on the temperature distribution through the thickness of CNTRC cylinder.

6. REFERENCES

- Alibeigloo, A., and K. M. Liew. "*Thermoelastic Analysis Of Functionally Graded Carbon Nanotube- Reinforced Composite Plate Using Theory Of Of Elasticity"* Compos Struct 106: 873-881
- Hu, N., H. Fukunaga, C. Lu, M. Kameyama, and B. Yan. 2005;"*Prediction Of Elastic Properties Of Carbon Nanotube Reinforced Composites*." In Proceedings of the Royal Society of London A: Mathematical, Physical and Engineering Sciences. 461: 1685-1710. The Royal Society.
- Lau AKT, Hui D. 2002*; The Revolutionary Creation Of New Advanced Materials—Carbon Nanotube Composites,* Composites: Part B 33:263–77.

- Lei, Z. X., Kim Meow Liew, and J. L. Yu. 2013; *Buckling Analysis Of Functionally Graded Carbon Nanotube-Reinforced Composite Plates Using The Element-Free Kp-Ritz Method*., *Composite Structures* 98: 160-168.
- Lei, Z. X., Kim Meow Liew, and J. L. Yu. 2013; *Large Deflection Analysis Of Functionally Graded Carbon Nanotube-Reinforced Composite Plates By The Element-Free Kp-Ritz Method*, Computer Methods in Applied Mechanics and Engineering 256: 189-199.
- Liu YJ, Chen XL. 2003; *Evaluations Of The Effective Material Properties Of Carbon Nanotube-Based Composites Using A Nanoscale Representative Volume Element*, Mech Mater 35:69–81.
- Malekzadeh, P., Y. Heydarpour, MR Golbahar Haghighi, and M. Vaghefi. 2012; *Transient Response Of Rotating Laminated Functionally Graded Cylindrical Shells In Thermal Environment*, International Journal of Pressure Vessels and Piping 98: 43-56.
- Manchado, MA Lopez, L. Valentini, J. Biagiotti, and J. M. Kenny. 2005; *Thermal And Mechanical Properties Of Single-Walled Carbon Nanotubes–Polypropylene Composites Prepared By Melt Processing*, *Carbon* 43:1499-1505.
- Moradi-Dastjerdi, Rasool, Mehrdad Foroutan, and Aminallah Pourasghar. 2013*; Dynamic Analysis Of Functionally Graded Nanocomposite Cylinders Reinforced By Carbon Nanotube By A Mesh-Free Method*, Materials & Design 44: 256-266.
- Ounaies, Z., C. Park, K. E. Wise, E. J. Siochi, and J. S. Harrison. 2003; *Electrical Properties Of Single Wall Carbon Nanotube Reinforced Polyimide Composites*, "Composites Science and Technology 63: 1637-1646.
- Qian D, Dickey EC, Andrews R, Rantell T. 2000; *Load Transfer And Deformation Mechanisms In Carbon Nanotube–Polystyrene Composites*, Appl Phys Lett 76:2868–70.
- Seidel, Gary D., and Dimitris C. Lagoudas. 2006; *Micromechanical Analysis Of The Effective Elastic Properties Of Carbon Nanotube Reinforced Composites*, Mechanics of Materials 38: 884-907.
- Shen, Hui-Shen. 2009;*Nonlinear Bending Of Functionally Graded Carbon Nanotube-Reinforced Composite Plates In Thermal Environments*, Composite Structures 91: 9-19.
- Shen, Hui-Shen. 2014; *Torsional Postbuckling Of Nanotube-Reinforced Composite Cylindrical Shells In Thermal Environments*, Composite Structures 116: 477-488.
- Thostenson ET, Ren Z, Chou TW. 2001;*Advances In The Science And Technology Of Carbon Nanotubes And Their Composites: A Review*, Compos Sci Technol 61:1899–912.
- Vodenitcharova, T., and L. C. Zhang. 2006; *Bending And Local Buckling Of A Nanocomposite Beam Reinforced By A Single-Walled Carbon Nanotube*, International journal of solids and structures 43: 3006-3024.
- Wang, Zhen-Xin, and Hui-Shen Shen. 2011; *Nonlinear Vibration Of Nanotube-Reinforced Composite Plates In Thermal Environments*, Computational Materials Science 50: 2319-2330.

- Wuite, J., and S. Adali. 2005; *Deflection And Stress Behaviour Of Nanocomposite Reinforced Beams Using A Multiscale Analysis*, Composite structures 71: 388-396.
- Yang, Shin-Yi, Wei-Ning Lin, Yuan-Li Huang, Hsi-Wen Tien, Jeng-Yu Wang, Chen-Chi M. Ma, Shin-Ming Li, and Yu-Sheng Wang. 2011; *Synergetic Effects Of Graphene Platelets And Carbon Nanotubes On The Mechanical And Thermal Properties Of Epoxy Composites*, Carbon. 49: 793-803.
- Yasmin, Asma, and Isaac M. Daniel. 2004; *Mechanical And Thermal Properties Of Graphite Platelet/Epoxy Composites*, Polymer 45: 8211-8219.
- Zhang, L. W., Z. X. Lei, K. M. Liew, and J. L. Yu. 2014; *Large Deflection Geometrically Nonlinear Analysis Of Carbon Nanotube-Reinforced Functionally Graded Cylindrical Panels*, Computer Methods in Applied Mechanics and Engineering 273: 1-18.
- Zhu, Ping, Z. X. Lei, and Kim Meow Liew. 2012; *Static And Free Vibration Analyses Of Carbon Nanotube-Reinforced Composite Plates Using Finite Element Method With First Order Shear Deformation Plate Theory*, Composite Structures 94: 1450-1460.
- Reddy JN. 2006 *An introduction to the finite element method*. 3rded.newyork: McGraw-Hill higher education,

NOMENCLATURE

$E_{11}^{cn}, E_{22}^{cn}, G_{12}^{cn}, E_m, G_m$: young's modules, shear modulus of carbon nanotube and matrix, respectively

$k_{cn}, \alpha_{ij}^{cn}, k_m, \alpha_m$: thermal conductivity and coefficient of thermal expansion of CNT and matrix, respectively

V_{cn}, V_m : CNTs and matrix volume fraction, respectively

$\eta_i \left(i = 1,2,3\right)$: CNT efficiency parameters

P : aspect ratio of CNTs

R_k : interface thermal resistance between CNT and matrix

$\sigma_i \left(i = r,\theta,z\right)$: normal stress

$\varepsilon_i \left(i = r,\theta,z\right)$: normal strains

$\gamma_{ij} \left(i = r, j = z\right)$: shear strain

$k_i \left(i = r, z\right)$: thermal conductivity in r and z direction

T : temperature

hc : convection heat transfer coefficient

λ : virtual displacement

φ : shape function

K : stiffness matrix

d : displacement vector

R : force vector

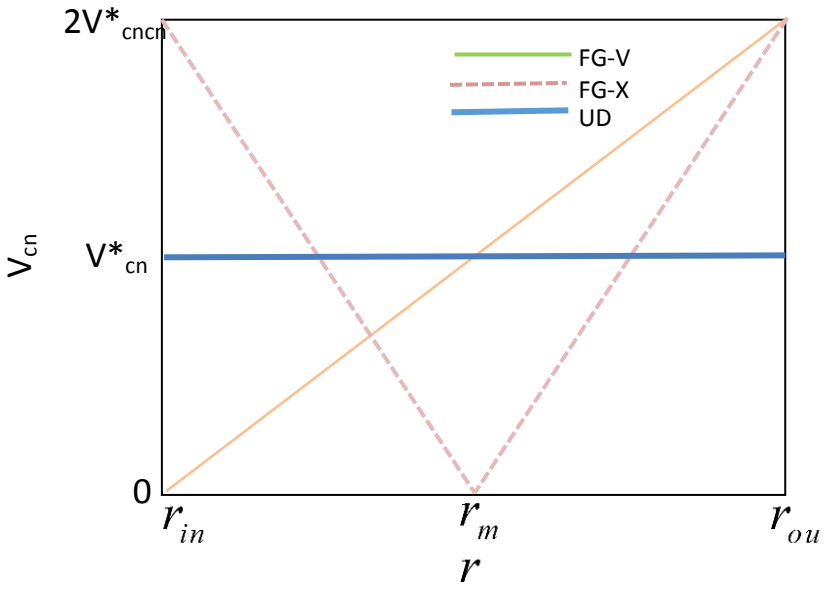

Figure 1. Distribution of CNT volume fraction through the radial direction for kinds of FG_V, FG_X and UD.

Table 1. Mechanical and thermal properties of CNT and polymer matrix [22].

	Carbon nanotube	*Polymer matrix*		η_i	p	R_k
$E_{11}^{cn}(TPa)$	5.6466	$E^m(GPa)$	2.1	$\eta_1 = 0.149$	350	$8\times10^{-8} m^2 k/w$
$E_{22}^{cn}(TPa)$	7.0800			$\eta_2 = 0.934$		
$E_{33}^{cn}(TPa)$	7.0800			$\eta_3 = 0.934$		
$G_{12}^{cn}(TPa)$	1.9445					
$G_{13}^{cn}(TPa)$	1.9445					
ν_{12}^{cn}	0.175		0.34			
$\rho^{cn}(gr/cm^3)$	1.4		1.5			
$K_z^{cn}(W/mK)$	3000	K^m	5			
$K_r^{cn}(W/mK)$	100					
$\alpha_r^{cn}(1/K)$	5.1682×10^{-6}					
$\alpha_z^{cn}(1/K)$	3.4584×10^{-6}					

Table 2. Comparison of dimensionless central deflection $\overline{w}$ for CNTRC square plate with two kinds of functionally Graded and UD of CNT distribution under the effect of uniform pressure($p_0=-1\times10^5 N/m^2$).

V_{cn}^*	$\frac{a}{h}$	Distribution kind	$\overline{W}$ (present)	$\overline{W}$ (Ref.[ ])
0.11	10	UD	2.229×10^{-3}	2.228×10^{-3}
		FG_V	2.353×10^{-3}	2.351×10^{-3}
		FG_X	2.111×10^{-3}	2.109×10^{-3}
	20	UD	1.340×10^{-3}	1.339×10^{-3}
		FG_V	1.595×10^{-3}	1.593×10^{-3}
		FG_X	1.151×10^{-3}	1.150×10^{-3}
0.17	10	UD	1.413×10^{-3}	1.412×10^{-3}
		FG_V	1.488×10^{-3}	1.486×10^{-3}
		FG_X	1.319×10^{-3}	1.318×10^{-3}
	20	UD	8.563×10^{-3}	8.561×10^{-3}
		FG_V	1.022×10^{-2}	1.021×10^{-2}
		FG_X	7.293×10^{-3}	7.290×10^{-3}

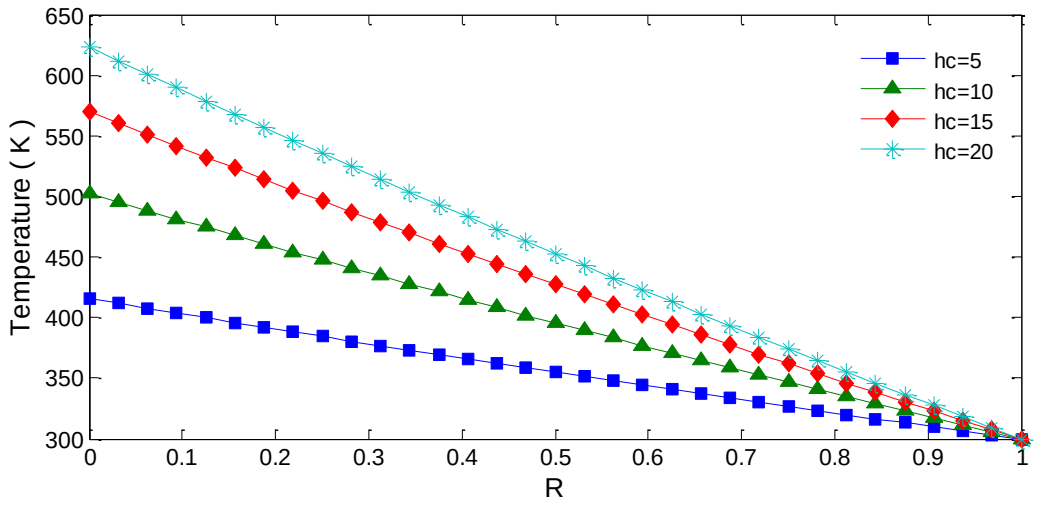

Figure 2. Through the radius distribution of temperature with different values of hc for CNTRC cylinder With FG_V .

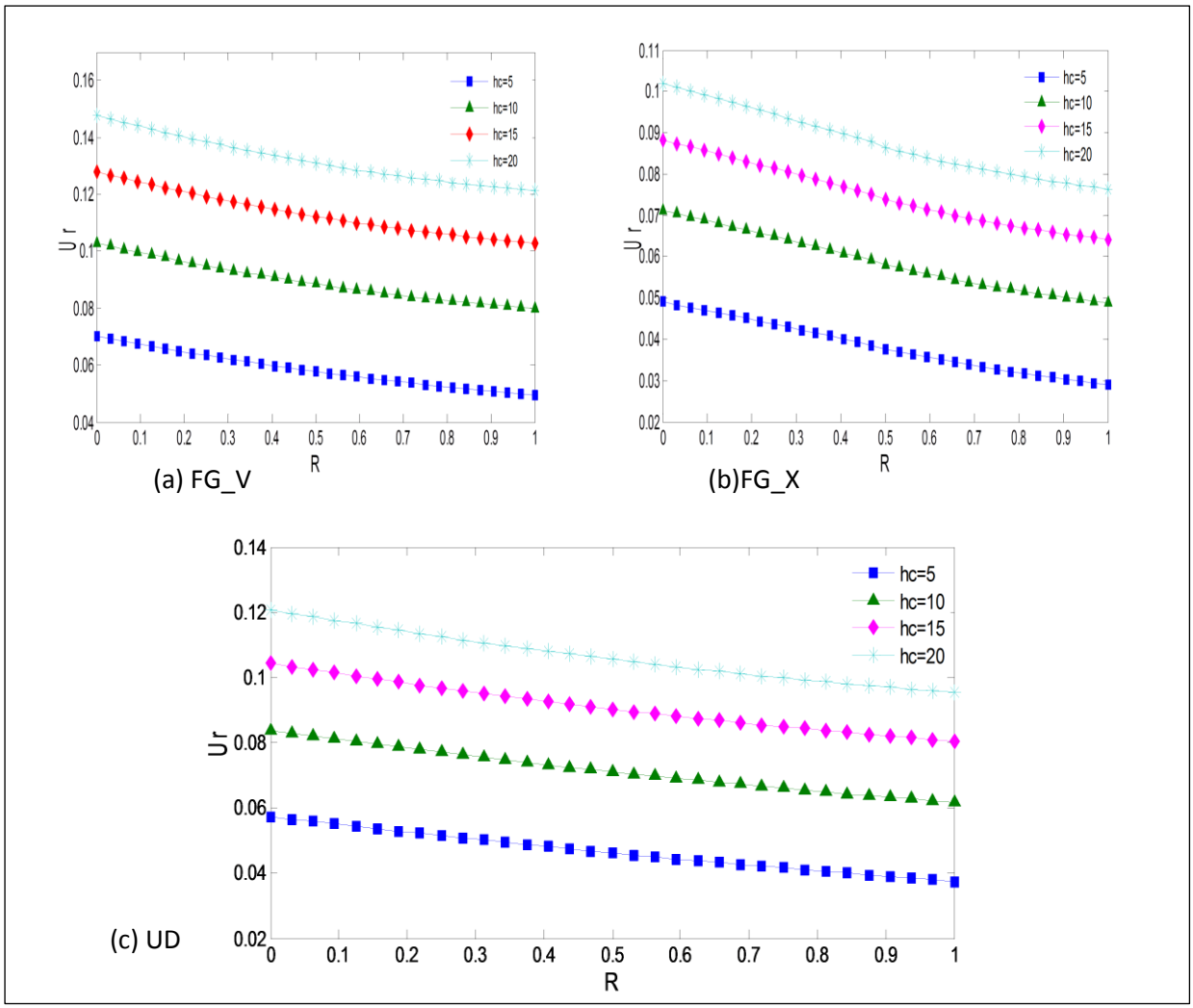

Figure 3. Through the radius distribution of radial displacement for clamped-clamped CNTRC cylinder.

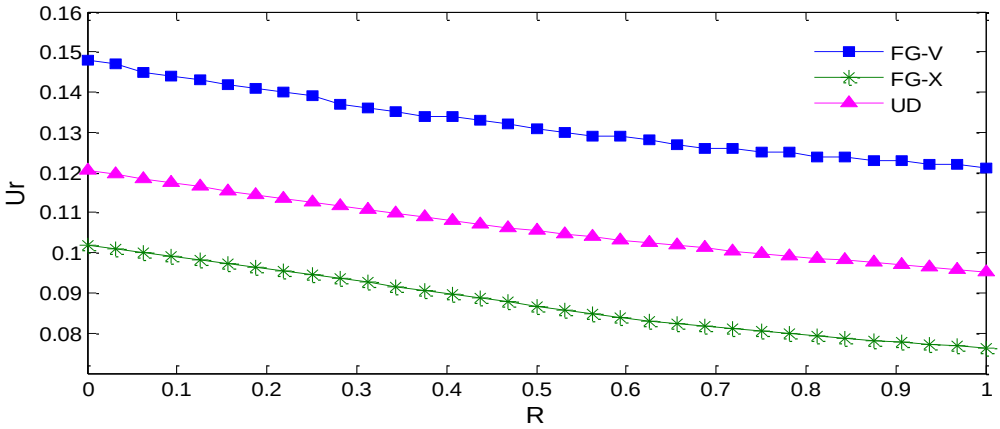

Figure 4. Through the radius distribution of radial displacement for clamped-clamped with different kinds of CNT distribution.

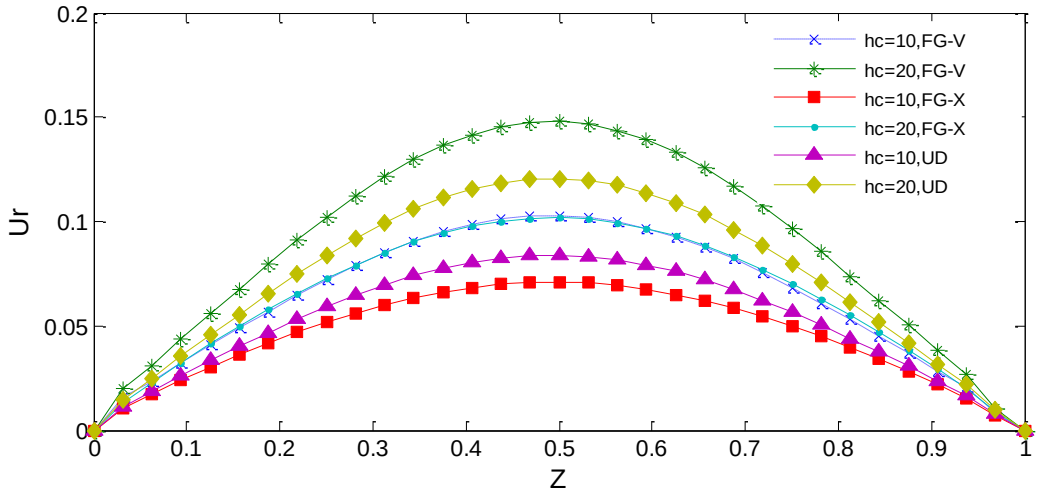

Figure 5. Through the longitudinal distribution of radial displacement for clamped-clamped CNTRC cylinder for different types of CNT distribution.

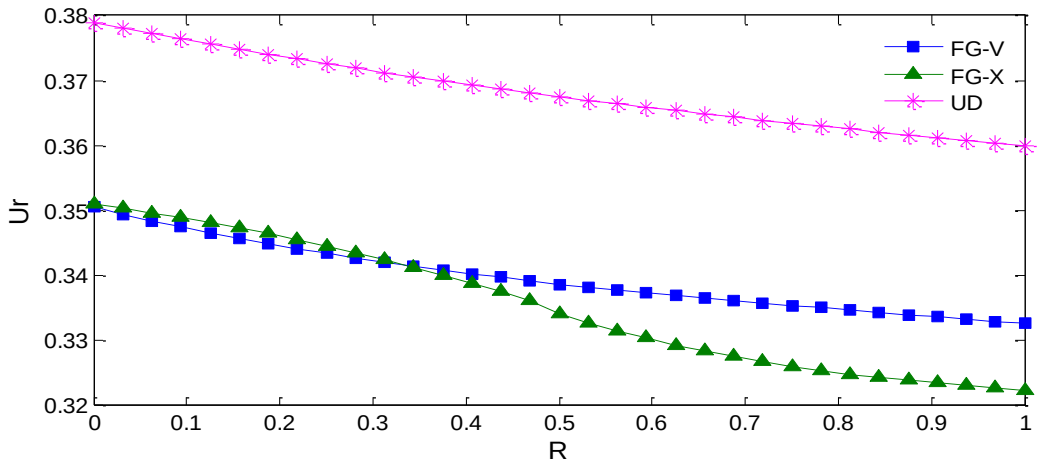

Figure 6. Through the radius distribution of radial displacement for clamped-free with different kinds of CNT distribution and hc=20(W/m^2K).

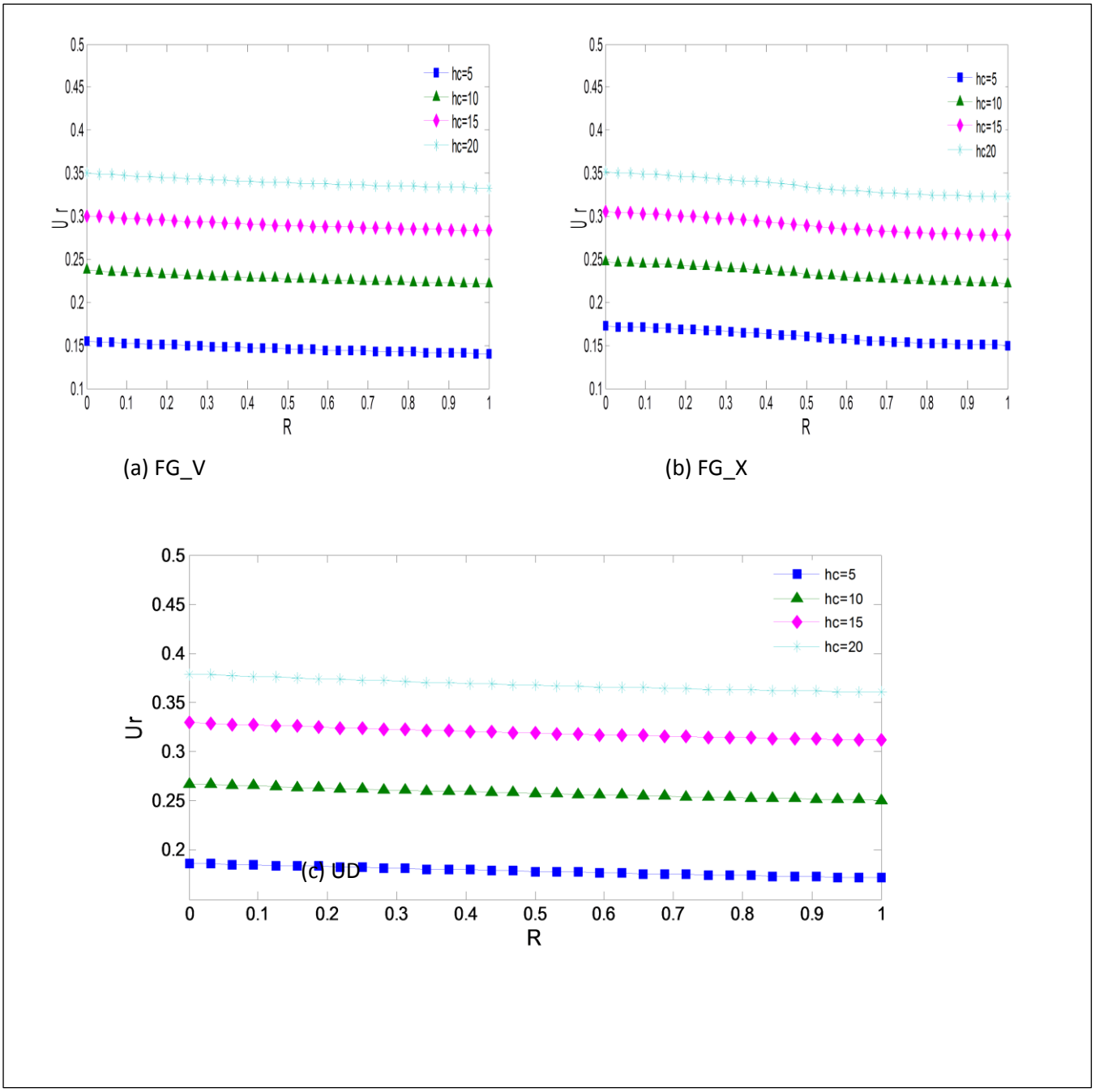

Figure 7. Through the radius distribution of radial displacement for clamped-free CNTRC cylinder.

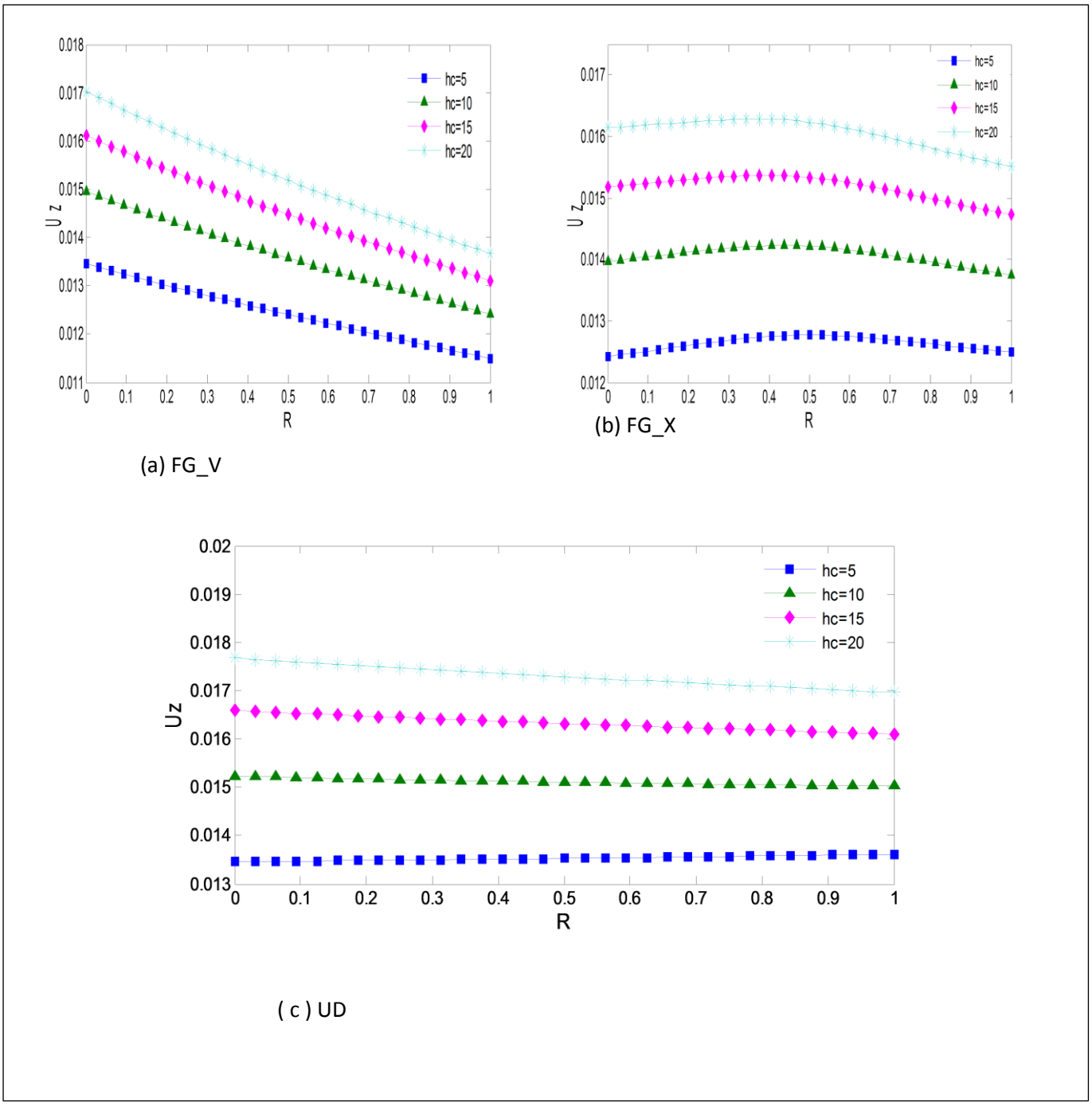

Figure 8. Through the radius distribution of longitudinal displacement for clamped-free CNTRC cylinder.